Implications of back-and-forth motion and powerful propulsion for spirochetal invasion

Keigo Abe[1], Toshiki Kuribayashi[1], Kyosuke Takabe[1**], and Shuichi Nakamura[1*]

[1]Department of Applied Physics, Graduate School of Engineering, Tohoku University, 6-6-05 Aoba, Aoba-ku, Sendai 980-8579, Japan

*Corresponding Author: Shuichi Nakamura, naka@bp.apph.tohoku.ac.jp, Tel: +81-22-795-5849

**Present address: Faculty of Life and Environmental Sciences, University of Tsukuba, Tsukuba 305-8572, Japan

Abstract

The spirochete *Leptospira* spp. can move in liquid and on a solid surface with two periplasmic flagella (PFs), and the motility is essential virulence factor for the pathogenic species. Although the fact that mammals are infected with the spirochete through wounded dermis imply the importance of behaviors on the boundary with such viscoelastic milieu, how the leptospiral pathogenicity involves motility remains unclear. We used the glass chamber containing a gel area adjoining the leptospiral suspension to resemble host dermis exposed to contaminated water and analyzed the motility of individual cells at the liquid-gel border. Insertion of one end of the cell body to the gel increased switching of the swimming direction. We also measured the swimming force of *Leptospira* by trapping single cells using optical tweezer, showing that they can produce ~17 pN, which is ~30 times of the swimming force of *Escherichia coli*. The force-speed relationship suggested the load-dependent force enhancement and showed that the power (the work per unit time) for the propulsion is ~3.1×10^{-16} W, which is two-order larger than the propulsive power of *E. coli*. Powerful, efficient propulsion of *Leptospira* with back-and-forth movements enabling them to explore invasion routes could facilitate percutaneous infection.

Introduction

Motility is a crucial virulence factor for pathogenic bacteria[1]. For example, a motility-deficient mutant of *Vibrio cholerae* is attenuated due to the decreased invasion efficiency to epithelium[2]. In some flagellated bacteria, not only motility but also the flagella themselves are essential as a adhesin, and *Salmonella* Enteritidis attaches on the host tissue via peritrichous flagella, resulting in colonization and clinical outcomes[3]. Although spirochetes, such as *Borrelia burgdorferi* (the Lyme disease)[4] and *Brachyspira hyodysenteriae* (swine dysentery)[5], also utilize motility in any steps of infection, since their flagella exist beneath the outer membrane so called periplasmic flagella (PFs), the spirochetal flagella are not involved in pathogenicity directly. Instead, improvement of swimming ability[6] and diverse adherence[7] in viscoelastic environments are believed to be responsible for their colonization and dissemination within hosts.

The genus *Leptospira* is a member of spirochetes, and the pathogenic species cause a worldwide zoonosis leptospirosis. Pathogenic *Leptospira* cells are maintained in the proximal renal tubules of the reservoir rodents. Urinary from such maintenance host shed the spirochetes into environments, and many mammals including human are percutaneously infected by contact with the contaminated soil and water[8,9]. *Leptospira* spp. have a right-handed spiral cell body and exhibit curvatures at both ends of the cell body (Fig. 1A). The

spirochete can swim in liquid and crawl on a surface using two PFs (one PF/cell end) (Fig. 1B), and the morphology of the cell ends changes between spiral and hook shapes frequently: An asymmetric configuration showing spiral and hook shapes at the anterior and posterior cell ends, respectively, propels the cell unidirectionally (Fig. 1B)[10–13]. As with other motile species, the motility of *Leptospir*a spp. are closely related to their pathogenicity[14,15], but how it practically works as a virulence factor in the spirochete remains unclear.

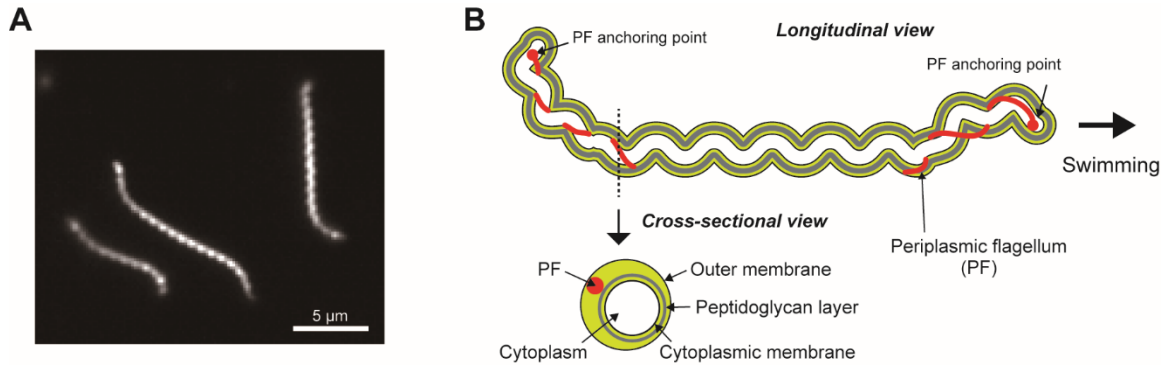

Fig. 1. Morphology of *Leptospira*. (A) Dark-field micrograph of *Leptospira kobayashii*. (B) Schematic diagram of the cell structure of *Leptospira* spp.; a swimming cell exhibiting the spiral anterior end (right side of the diagram) and hook-shaped posterior end (left side) is illustrated.

As a possible scenario for the motility dependence of the *Leptospira* pathogenicity, we recently showed that the spirochete increased the frequency of changing the swimming direction with the elevated viscosity of polymer solutions, and the resultant limitation of their net migrations could be involved in accumulation of the spirochete in epithelial mucosa *in vivo*[12]. In this study, hypothesizing the significance of the phenomenon observed in polymer solution for percutaneous infection of *Leptospira*, we investigated their behaviors at the border of liquid and gel phases resembling the skin dermis exposed to the contaminated environmental water. Furthermore, we expected the necessity of large propulsive force for the invasion and performed force measurements of swimming spirochetes using optical tweezer. Our experiments showed that the enhancement of swimming reversal when only one end of the cell body is inserted to gel, and much larger swimming force of *Leptospira* than the known values of exoflagellated bacteria. The results suggest that powerful and efficient swimming with the repeated trial-and-error allows *Leptospira* for having an easy passage for penetration through host dermis.

Results

Swimming reversal. To investigate the leptospiral behaviors when penetrating viscoelastic environments, we observed the spirochetes using a flow chamber containing liquid medium and agar that are contiguous (Fig. 2A). *Leptospira* cells show relatively smooth swimming in liquid (Figs. 2B left and 2C left). In contrast, inserting one end of the cell body to agar, they frequently changed the swimming direction (Figs. 2B right and 2C right). Significant difference in reversal frequencies between cells in liquid and at the liquid-agar border are shown in Fig. 2D. Video 1 shows that a *Leptospira* cell succeeds to penetrate agar after several back-and-forth movements. Enhancement of swimming reversal at the liquid-agar border was also observed in different species of *Leptospira* (Video 2 for *L. interrogans* and Video 3 for *L. biflexa*), thus suggesting that the phenomenon would be common among the genus. For pathogenic species, exploring easier route in dermis (e.g., structurally disturbed parts due to deep injury) by such "trial and error" could facilitate percutaneous invasion (Fig. 2E).

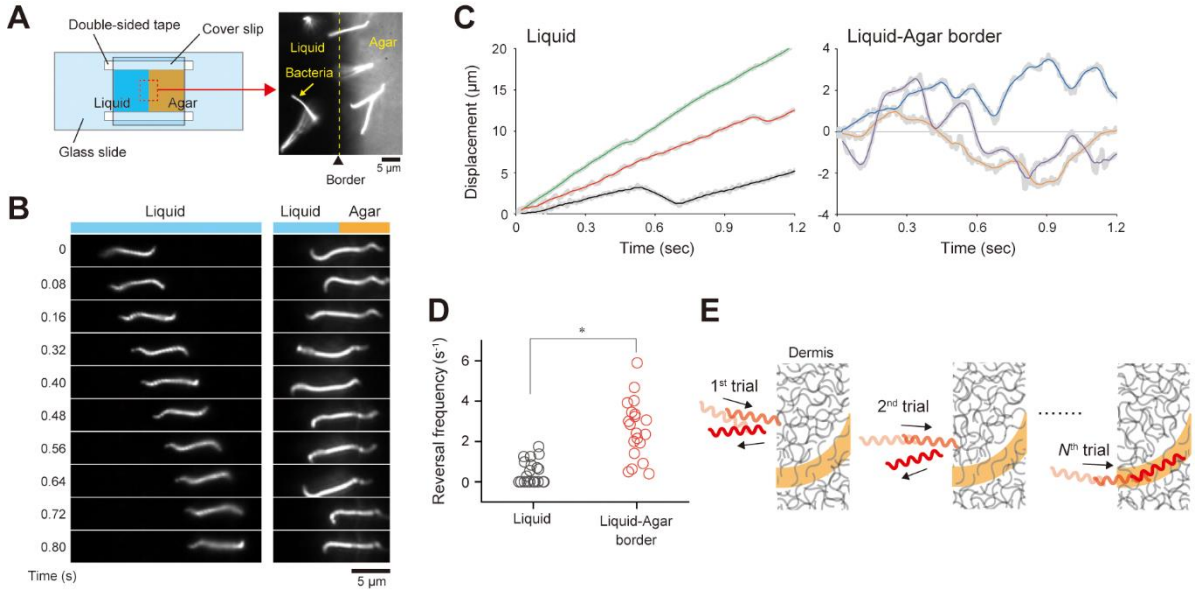

Fig. 2. Swimming reversal. (A) Illustration of a flow chamber in which liquid and agar areas are contiguous. The microscopic image shows the liquid-agar border. Bacteria swam in liquid at the beginning of the experiment and then penetrated the agar area. (B) Time courses of the cell-movements observed in liquid (left) and at the liquid-agar border (right). (C) Displacements of individual cells. Example data obtained from three *L. kobayashii* cells are shown each in liquid and the border. Thick gray lines indicate raw data obtained by determining cell positions at 4-ms intervals, and thin colored lines are the results of 12-data-point moving average. (D) Comparison of the reversal frequency determined from the cell displacement data. The results of liquid contain zero, i.e., no reversals occurred during observation. Mann-Whitney U test showed significant difference (*$P < 0.05$); n = 24 cells for liquid, and n = 20 cells for the border. (E) A plausible contribution of frequent swimming reversals for invasion. Back-and-forth movements give the cell chance to find an easier invadable route in heterogeneous dermis structure (orange). Video 1 demonstrates "trial-and-error" at the liquid-agar border by swimming reversals.

Force measurement for the *Leptospira* swimming. For measurement of the swimming force of *Leptospira*, we trapped a microbead attached to a swimming cells with optical tweezer (Figs 3A-B). By considering balance of the swimming force (F) with the trapping force (F_{trap}) and the drag force (F_{drag}) exerted on the bead, $F = F_{trap} + F_{drag}$ (Fig. 3C), the bead displacements were calibrated to swimming force (Fig. 3D and Video 4). The swimming force increased with the cell displacement and reached the saturation where the cell is stalled by restoring force of the laser trap. The stall force largely differed among the measured cells, and the averaged force-time curve showed the stall force of 16.6 ± 2.2 pN (mean ± standard error; n = 24 cells) (Fig. 4A). A model experiment in which a tungsten coil mimicking the shape of *Leptospira* was rotated in a rotational magnetic field showed that 2.2 pN is required at most for penetrating agar resembling skin dermis[16]. Our results showed that actual leptospires can produce swimming force about eight times as much as the previous model prediction. Furthermore, the swimming force of *Leptospira* is ~30 times as much as that of *E. coli* (~0.6 pN)[17].

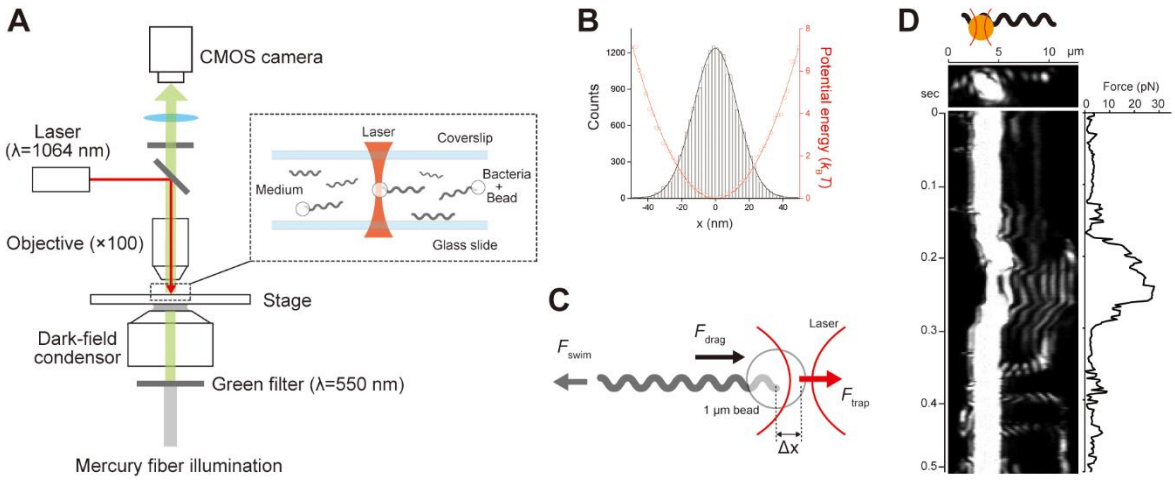

Fig. 3. Swimming force measurement. (A) A dark-field microscope equipped with optical tweezer. (B) The distribution of the positions of a 1-μm bead trapped by optical tweezers (histogram) and the estimated potential profile (red circles). The black and red lines indicate the results of curve fitting by the Gaussian distribution and harmonic function, respectively. Spring constants were measured in each chamber, and 16-36 pN/μm were used. (C) Force balance in a swimming cell trapped by optical tweezer. See Methods for details. (D) Time course of the bead position that is attached to a leptospiral cell and is trapped by optical tweezer. The left upper schematic represents a trapped *Leptospira* via a 1-μm bead; the left lower panel is a kymograph showing bead movement with the leptospiral swimming. The right panel indicates the time course of the force estimated from the bead movement. See also Video 4.

Force-speed relationship. The relationship between force and speed was obtained from the force-time plots, showing that swimming forces linearly decrease with the increased swimming speed (Fig. 4B). The force-speed curves suggest that *Leptospira* could vary the propulsive force depending on load exerted on the cell, that is viscous drag and trapping force. Namely,

the observed variation of the slope in the force-speed curves implies the difference of the load responsivity among cells. We calculated the work per unit time, $F \cdot v$, for the *Leptospira* propulsion using the measured values (Fig. 4C). The propulsive power of *Leptospira* is in the range from 1×10^{-16} to 7×10^{-16} W, which is two order larger than that of *E. coli* (5.8×10^{-18} W)[17]. These results suggest that *Leptospira* can produce large force with maintaining high efficiency when penetrating to gel-like viscous materials.

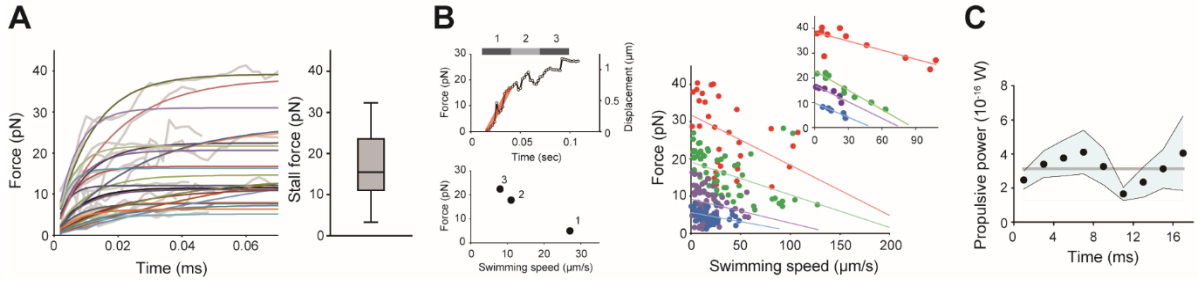

Fig. 4. Swimming force. (A) Time courses of the swimming force obtained from 24 *L. kobayashii* cells. Gray and colored lines indicate the measured force curves and the results of exponential curve fitting, respectively. All of the force curves are shown in Supplementary Fig. S1 separately. The right panel shows the stall forces determined by the curve fitting; the boxes show the 25th (the bottom line), 50th (middle), and 75th (top) percentiles, and the vertical bars show the standard deviation. (B, left) Conversion from the force-time plot to the force-speed relationship, which is explained using an example trace extracted from *A*. The data plotted in the force-time plot were separated with an equal time interval, and the averaged forces of each bin were plotted against the average speeds determined by line fitting as shown in red in the upper panel. (right) The force-speed curve obtained from 24 cells were classified into four groups by stall force: <10 pN (blue), 10-20 pN (purple), 20-30 pN (green), and >30 pN (red). The colored lines are the regression lines fitted to each group. Example data extracted from each group are shown in the inset. (C) Time course of the power of the *Leptospira* swimming calculated by $F \cdot v$. Black dots and the blue band indicate average values at each time point (n = 24 cells) and standard error, respectively. The horizontal gray line indicates the average power of the entire time course (3.1×10^{-16} W).

Discussion

Although the relevance of flagella and motility to bacterial pathogenicity is known, their roles differ for species, and the motility-dependent pathogenicity of bacteria is not fully elucidated. We focused on the association of motility with invasion of the *Leptospira* spirochete. Our biophysical experiments revealed that back-and-forth movement of *Leptospira* is enhanced when only one of the cellular ends is exposed to high viscosity and that the spirochete can produce much larger swimming force than exoflagellated bacteria. Frequent changes in the swimming direction allow the cell to search environments and to come across preferable entrances. The observed trial-and-error behavior will be significance for infection through dermis, because such heterogeneous fibrous structures may obstruct the spirochetal invasion even though they have high propulsion. The viscosity-dependent reversal was observed in

both pathogenic and non-pathogenic species, implying that leptospires can penetrate the dermis regardless of pathogenicity in terms of kinematics. However, since the motility of the non-pathogenic *L. biflexa* is lost immediately after exposure to physiological osmotic condition[18], dissemination within the host will not be allowed.

Enhancement of swimming reversal has been observed in polymer solutions, where the entire spirochetal body was exposed to changes in environmental viscosity or viscoelasticity[12]. However, we showed that swimming reversal is increased by that very limited part of the cell body is placed in viscoelastic milieu. Given that the torque for rotating the spiral body of *Leptospira* is produced by PFs residing at both cellular ends, the two PFs should rotate cooperatively for propelling the cell. In this context, our results suggest some sort of signal transduction between cell ends. Thus, one of the remaining issues is the mechanism by which leptospires sense the viscoelastic change at one end and transmit the mechanical signal to the other end rapidly (< 1 s at the latest; see Video 5 for the rapid reversal). It is known that coordinated rotations observed between *E. coli* flagellar motors depend on diffusion of the phosphorylated chemotactic signaling protein CheY-P[19]. *Leptospira* spp. also possess several CheY homologues[20], but its diffusion is too slow to transmit signals from one end to the other along ~20 μm: CheY with a diffusion coefficient D = 10 μm^2/s[19] is estimated to take t = 40 s for diffusing x = 20 μm using $t = x^2/D$. Instead, the relatively stiff protoplasmic cylinder might be a possible medium for mechanical signal transduction[11,21]. Elucidating the coordinated control mechanism of PFs will be a future subject.

The measured swimming force of *Leptospira* was ~30 times larger than that of *E. coli*[17]. Such greater force generation by the spirochete could be attributed to drag coefficients and high toque motor. Hydrodynamic studies in low Reynolds number using the resistive force theory showed that drag force exerted on a spherical cell body with a spiral, thin body that rotate at ω_{Lep} and translate at v_{Lep} in liquid is calculated by $F_{\mathrm{Lep}} = \alpha_{\mathrm{Lep}} v_{\mathrm{Lep}} + \beta_{\mathrm{Lep}} \omega_{\mathrm{Lep}}$, where α_{Lep} and β_{Lep} are drag coefficients for a spiral cell body[6,11,22]. Similarly, drag force on a externally flagellated bacteria assumed by a spherical body with a flagellum is given by $F_{\mathrm{Efb}} = \alpha_{\mathrm{Efb}} v_{\mathrm{Efb}} + \beta_{\mathrm{Ef}} \omega_{\mathrm{Ef}}$, where α_{Efb} is the sum of drag coefficients for the translating spherical cell body α_{Cell} and filament α_{Ef} ($\alpha_{\mathrm{Efb}} = \alpha_{Cell} + \alpha_{\mathrm{Ef}}$) and β_{Ef} is the drag coefficient for the flagellar rotation; $v_{\mathrm{Efb}}$and ω_{Ef} are the swimming speed and the flagellar rotation rate, respectively[23]. These drag coefficients depend on geometrical parameters such as the length and width of a cell body, wavelength and amplitude of a helix, and fluid viscosity (see Methods). Calculations using morphological parameters of *L. biflexa*[11] and *E. coli* give α_{Lep} = -0.056 pN·s/μm, β_{Lep} = 0.002 pN·s, α_{Ef} = -0.02 pN·s/μm, and β_{Ef} = 0.0003 pN·s, thus indicating that drag coefficients for the leptospiral body is larger than those for *E. coli*. Despite such large

drag coefficients, the swimming speed (~20 μm/s) and cell-body rotation rates (>100 Hz) of *Leptospira* spp. are comparable to those of *E. coli*[17]. Cryo-electron microscopy revealed that, in comparison with conventional flagellar motors e.g., of *E. coli* and *Salmonella* spp., the rotor ring of the spirochetal flagellar motor is larger[24], and greater number of torque generators (stator units) are assembled[25]. Thus, large swimming force of *Leptospira* could be provided by high torque motor that can rotate the heavy cell body. Since the cell morphology, the motor structure, and the swimming velocity are very similar among different species of *Leptospira*[18,25], the spirochetal genus would be powerful swimmers in common.

The stall force was uneven among the measured cells (Fig. 4A). At high load, the motor torque of the external flagellum depends on the number of the stators and the input energy ion motive force (IMF)[26]. Because stable incorporation of the full number of the stator units to the motor has been shown in *Leptospira* spp. by electron cryo-tomography[25], the difference in the IMF is a possible cause of the varied stall force. Furthermore, since an intimate contact between PFs and cell membranes is thought to be important for the spirochetal swimming[27], the PF-membrane interaction or morphological differences of PFs, such as length, could affect the propulsion.

The force-speed relationship (Fig. 4B) showed that the swimming force decreases with the increased speed. This result suggests the mechanism by which the spirochete varies the propulsive output in response to the change in load, producing larger force at high load. The load-dependent assembly of the stator units is observed in the flagellar motors of *E. coli* and *Salmonella*[28–31]. Although such stator dynamics seems to be implausible for the *Leptospira* motor as referred above, leptospires may adjust their propulsive force through another mechano-sensing mechanism, allowing the spirochete to invade highly viscous environments while maintaining large power output.

Methods

Bacteria and media. The saprophytes *Leptospira biflexa* strain Patoc I and *Leptospira kobayashii*[32], and the pathogenic species *Leptospira interrogans* serovar Manilae strain UP-MMC-NIID[33] were grown at 30°C for 4 days in Ellinghausen-McCullough-Johnson-Harris (EMJH) liquid medium with 10% bovine serum albumin until the stationary phase. Potassium phosphate buffer (20 mM, pH7.4) was used as motility medium[12].

Measurement of swimming reversal. The *Leptospira* culture was centrifuged at 1,000 G for 10 min at 23°C, and the precipitated cells were resuspended in the motility medium without dilution. The bacterial suspension was infused to a flow chamber that was made by sticking a

coverslip and a glass slide with double-sided tape (90 μm in thickness) and contained 0.2% agar so that agar and liquid area are contiguous in the chamber (Fig. 2A). The liquid-agar border was observed with a dark-field microscope (BX53, 40× objective, 5× relay lens, Olympus, Tokyo, Japan), and behaviors of cells inserting one end of the cell body into agar were recorded with the CMOS camera at 250 Hz.

The swimming reversal is measured by tracing the cellular centroid in general[34,35]. However, morphology of the *Leptospira* cell changes frequently, thus affecting the consistency between the centroid displacement and the actual cell movement (Supplementary Fig. S2). To avoid the false recognition of the reversal, the positions of the both ends of the cell body were determined with the centroid, and simultaneous displacements of the three points were recognized as cell movements (Fig. S2A). Swimming speeds were measured by line fitting to the time courses of the cell displacements at an interval of 0.1 s, and <1 μm/s was judged as "pausing". The reversal frequency was determined by normalizing the number of the reversals (N_{rev}) by the observation time (t), i.e., N_{rev}/t. The data were analyzed with ImageJ (National Institutes of Health, Rockville, MD) and programs originally developed using LabVIEW 2014 (National Instruments).

Measurement of swimming force. A dark-field microscope (BX50, Olympus, Tokyo, Japan) that is essential for observing a thin leptospiral cell body (~140 nm in diameter) was equipped with an optical tweezer (Fig. 2A). The cell suspension prepared by the same procedure as the reversal measurement was mixed with 1.0-μm carboxyl latex beads (ThermoFisher Scientific, Waltham, MA) and was incubated at 23°C for 10 minutes. The mixture was infused to the glass-made chamber, and spontaneous bead attachments to swimming cells were observed. The attached bead was trapped by 1064-nm semiconductor laser (TLD001, Laser Diode Driver, Thorlabs Inc. Newton, NJ) through a 100× oil immersion objective lens (UPlanFLN, Olympus, Tokyo, Japan), and the bead movement was recorded with a CMOS video camera (acA800-510um, Basler, Ahrensburg, Germany) at frame rate of 60 Hz. The numerical aperture of the objective was adjusted with the objective-lens aperture so as to perform dark-field observation and laser trapping simultaneously. The recorded movie was analyzed with a custom-made program developed using LabVIEW 2014 (National instruments, Austin, TX) for determining the bead displacement.

Displacement of a trapped bead (Δx) can be calibrated to a restoring force of optical tweezer (F_{trap}) using the equation $F_{trap} = k\Delta x$, where k is a spring constant. The values of k were determined in each flow chamber by trapping a bead free from cells and analyzing its positional fluctuation as follows. The positional distribution of the trapped bead shows a

gaussian distribution $f(x) \propto exp(-x^2/2\sigma^2)$, where σ is the standard deviation (Fig. 2B, black line), obeying Boltzmann's law $P(x) \propto exp(-\Delta U/k_B T)$, where ΔU is the potential energy, k_B is the Boltzmann constant (1.38 $\times 10^{-23}$ J/K), and T is the absolute temperature (296 K), namely, $\Delta U = (k_B T/2\sigma^2)x^2$ (Fig. 2B, red line). Meanwhile, since the thermal fluctuation of the bead captured by a spring with k can be described by the harmonic function $U(x) = 1/2\, kx^2$, $k = k_B T/\sigma^2$. The swimming force was determined using F_{trap} and F_{drag} (Fig. 2C). When the bead with a diameter of r is moved at a speed of v (i.e., swimming speed of the cell) in a solution with a viscosity of μ, $F_{drag} = 6\pi\mu r \cdot v$, where $6\pi\mu r$ is a drag coefficient given by Stokes' low. The viscosity of the motility medium was measured with a tuning-fork-type viscometer (SV-1A, A&D, Tokyo, Japan), giving 0.8 mPa×s at 23°C.

Drag coefficients. Drag coefficients for the spirochete and externally flagellated bacterium are calculated as described previsouly[11,23]. For the *Leptospira* cell, the protoplasmic cylinder lacking bending at the cell ends was assumed:

$$\alpha_{\mathrm{Lep}} = C_{Lep}\left(8\pi^2 {r_{Lep}}^2 + {p_{Lep}}^2\right);$$
$$\beta_{\mathrm{Lep}} = -2C_{Lep}\pi {r_{Lep}}^2 p_{Lep};$$
$$C_{Lep} = 2\pi\mu L_{Lep}/\left\{\left(\log[d_{Lep}/2p_{Lep}] + 0.5\right)\left(4\pi^2 {r_{Lep}}^2 + {p_{Lep}}^2\right)\right\}.$$

Here, r_{Lep}, p_{Lep}, L_{Lep}, and $2d_{Lep}$ are the helix radius (0.09 μm), helix pitch (0.7 μm), length (20 μm), and diameter (0.14 μm) of the leptospiral cell body[11,36]. Drag coefficients for the externally flagellated bacterium that was assumed to consist of a spherical body and a helical filament, referring to the morphology of *Vibrio alginolyticus*[23], were calculated as follows:

$$\alpha_{Cell} = -6\pi\mu a\{1 - 0.2(1 - b/a)\};$$
$$\alpha_{\mathrm{Ef}} = C_{Ef}\left(8\pi^2 {r_{Ef}}^2 + {p_{Ef}}^2\right);$$
$$\beta_{\mathrm{Ef}} = -2C_{Ef}\pi r^2 p_{Ef};$$
$$C_{Ef} = 2\pi\mu L_{Ef}/\left\{\left(\log[d_{Ef}/2p_{Ef}] + 0.5\right)\left(4\pi^2 {r_{Ef}}^2 + {p_{Ef}}^2\right)\right\}.$$

Here, $2a$ and $2b$ are the diameter (0.8 μm) and length (1.92 μm) of the cell body, and r_{Ef}, p_{Ef}, L_{Ef}, and $2d_{Ef}$ are the helix radius (0.14 μm), helix pitch (1.58 μm), length (5.02 μm), and diameter (0.032 μm) of the flagellum. The medium viscosity μ was assumed to be 1 mPa×s.

References

1. Josenhans, C. & Suerbaum, S. The role of motility as a virulence factor in bacteria. *International Journal of Medical Microbiology* **291**, 605–614 (2002).
2. Guentzel, M. N. & Berry, L. J. Motility as a virulence factor for *Vibrio cholerae*. *Infect Immun* **11**, 890–897 (1975).

3. Olsen, J. E. *et al.* The role of flagella and chemotaxis genes in host pathogen interaction of the host adapted *Salmonella enterica* serovar Dublin compared to the broad host range serovar *S*.Typhimurium. *BMC Microbiology* **13**, 67 (2013).
4. Li, C., Xu, H., Zhang, K. & Liang, F. T. Inactivation of a putative flagellar motor switch protein FliG1 prevents *Borrelia burgdorferi* from swimming in highly viscous media and blocks its infectivity. *Mol. Microbiol.* **75**, 1563–1576 (2010).
5. Rosey, E. L., Kennedy, M. J. & Yancey, R. J. Dual *flaA1 flaB1* mutant of *Serpulina hyodysenteriae* expressing periplasmic flagella is severely attenuated in a murine model of swine dysentery. *Infect. Immun.* **64**, 4154–4162 (1996).
6. Nakamura, S., Adachi, Y., Goto, T. & Magariyama, Y. Improvement in motion efficiency of the spirochete *Brachyspira pilosicoli* in viscous environments. *Biophys. J.* **90**, 3019–3026 (2006).
7. Harman, M. W. *et al.* The heterogeneous motility of the Lyme disease spirochete in gelatin mimics dissemination through tissue. *PNAS* **109**, 3059–3064 (2012).
8. Adler, B. & de la Peña Moctezuma, A. *Leptospira* and leptospirosis. *Veterinary Microbiology* **140**, 287–296 (2010).
9. Picardeau, M. Virulence of the zoonotic agent of leptospirosis: still terra incognita? *Nat Rev Micro* **15**, 297–307 (2017).
10. Goldstein, S. F. & Charon, N. W. Multiple-exposure photographic analysis of a motile spirochete. *Proc. Natl. Acad. Sci. U.S.A.* **87**, 4895–4899 (1990).
11. Nakamura, S., Leshansky, A., Magariyama, Y., Namba, K. & Kudo, S. Direct measurement of helical cell motion of the spirochete leptospira. *Biophys. J.* **106**, 47–54 (2014).
12. Takabe, K. *et al.* Viscosity-dependent variations in the cell shape and swimming manner of *Leptospira*. *Microbiology* **163**, 153–160 (2017).
13. Nakamura, S. Spirochete flagella and motility. *Biomolecules* **10**, 550 (2020).
14. Lambert, A. *et al.* FlaA proteins in *Leptospira interrogans* are essential for motility and virulence but are not required for formation of the flagellum sheath. *Infect. Immun.* **80**, 2019–2025 (2012).
15. Xu, J., Koizumi, N. & Nakamura, S. Adhesivity and motility of a zoonotic spirochete: Implications in host-dependent pathogenicity. *bioRxiv* 2020.02.11.944587 (2020) doi:10.1101/2020.02.11.944587.
16. Ishibashi, Y., Han, Y.-H., Morisaki, H., Ishiyama, K. & Uehara, N. Swimming and invasion force estimations for *Leptospira* and its adhesion potential onto skin. *Journal of Water and Environment Technology* **11**, 341–354 (2013).

17. Chattopadhyay, S., Moldovan, R., Yeung, C. & Wu, X. L. Swimming efficiency of bacterium *Escherichia coli*. *Proc Natl Acad Sci U S A* **103**, 13712–13717 (2006).
18. Takabe, K., Nakamura, S., Ashihara, M. & Kudo, S. Effect of osmolarity and viscosity on the motility of pathogenic and saprophytic *Leptospira*. *Microbiol. Immunol.* **57**, 236–239 (2013).
19. Terasawa, S. *et al.* Coordinated reversal of flagellar motors on a single *Escherichia coli* cell. *Biophys J* **100**, 2193–2200 (2011).
20. Li, Z.-H. *et al.* Characterization of the *cheY* genes from *Leptospira interrogans* and their effects on the behavior of *Escherichia coli*. *Biochemical and Biophysical Research Communications* **345**, 858–866 (2006).
21. Kan, W. & Wolgemuth, C. W. The shape and dynamics of the *Leptospiraceae*. *Biophys. J.* **93**, 54–61 (2007).
22. Magariyama, Y. & Kudo, S. A Mathematical explanation of an increase in bacterial swimming speed with viscosity in linear-polymer solutions. *Biophysical Journal* **83**, 733–739 (2002).
23. Magariyama, Y. *et al.* Simultaneous measurement of bacterial flagellar rotation rate and swimming speed. *Biophys J* **69**, 2154–2162 (1995).
24. Beeby, M. *et al.* Diverse high-torque bacterial flagellar motors assemble wider stator rings using a conserved protein scaffold. *PNAS* **113**, E1917–E1926 (2016).
25. Raddi, G. *et al.* Three-dimensional structures of pathogenic and saprophytic *Leptospira* species revealed by cryo-electron tomography. *J. Bacteriol.* **194**, 1299–1306 (2012).
26. Nakamura, S. & Minamino, T. Flagella-driven motility of bacteria. *Biomolecules* **9**, 279 (2019).
27. Takabe, K., Kawamoto, A., Tahara, H., Kudo, S. & Nakamura, S. Implications of coordinated cell-body rotations for *Leptospira* motility. *Biochemical and Biophysical Research Communications* **491**, 1040–1046 (2017).
28. Tipping, M. J., Delalez, N. J., Lim, R., Berry, R. M. & Armitage, J. P. Load-dependent assembly of the bacterial flagellar motor. *mBio* **4**, e00551-13 (2013).
29. Lele, P. P., Hosu, B. G. & Berg, H. C. Dynamics of mechanosensing in the bacterial flagellar motor. *PNAS* **110**, 11839–11844 (2013).
30. Sato, K., Nakamura, S., Kudo, S. & Toyabe, S. Evaluation of the duty ratio of the bacterial flagellar motor by dynamic load control. *Biophysical Journal* **116**, 1952–1959 (2019).
31. Nord, A. L. *et al.* Catch bond drives stator mechanosensitivity in the bacterial flagellar motor. *Proc. Natl. Acad. Sci. U.S.A.* **114**, 12952–12957 (2017).

32. Vincent, A. T. *et al.* Revisiting the taxonomy and evolution of pathogenicity of the genus *Leptospira* through the prism of genomics. *PLOS Neglected Tropical Diseases* **13**, e0007270 (2019).
33. Koizumi, N. & Watanabe, H. Leptospiral immunoglobulin-like proteins elicit protective immunity. *Vaccine* **22**, 1545–1552 (2004).
34. Magariyama, Y. *et al.* Difference in bacterial motion between forward and backward swimming caused by the wall effect. *Biophys J* **88**, 3648–3658 (2005).
35. Son, K., Guasto, J. S. & Stocker, R. Bacteria can exploit a flagellar buckling instability to change direction. *Nature Physics* **9**, 494–498 (2013).
36. Goldstein, S. F., Buttle, K. F. & Charon, N. W. Structural analysis of the *Leptospiraceae* and *Borrelia burgdorferi* by high-voltage electron microscopy. *J. Bacteriol.* **178**, 6539–6545 (1996).

Acknowledgements We thank Toshiyuki Masuzawa for providing *Leptospira* strains. We also thank Shoichi Toyabe and Jun Xu for technical supports. This work was supported by the JSPS KAKENHI (18K07100 for SN).

Author contributions K.A., K.T. and S.N. planned the project; K.A., T.K., K.T. and S.N. carried out the experiments; K.A. and K.T. set up the optical system; K.A. and T.K. made programs for data analysis; K.A., T.K. and S.N. analyzed the data; K.A., T.K. and S.N. wrote the paper.

Competing interests The authors declare that they have no competing interests.

Data availability The data supporting the findings of this study are available from the corresponding author upon request.